

Ion-Channel Noise Places Limits on the Miniaturization of the Brain's Wiring

A. Aldo Faisal,^{1,*} John A. White,²
and Simon B. Laughlin¹

¹Department of Zoology
University of Cambridge
Downing Street
CB2 3EJ Cambridge
United Kingdom

²Department of Biomedical Engineering
Boston University
44 Cummington Street
Boston, Massachusetts 02215

Summary

The action potential (AP) is transmitted by the concerted action of voltage-gated ion channels. Thermodynamic fluctuations in channel proteins produce probabilistic gating behavior, causing channel noise. Miniaturizing signaling systems increases susceptibility to noise, and with many cortical, cerebellar, and peripheral axons <0.5 μm diameter [1–3], channel noise could be significant [4, 5]. Using biophysical theory and stochastic simulations, we investigated channel-noise limits in unmyelinated axons. Axons of diameter below 0.1 μm become inoperable because single, spontaneously opening Na channels generate spontaneous AP at rates that disrupt communication. This limiting diameter is relatively insensitive to variations in biophysical parameters (e.g., channel properties and density, membrane conductance and leak) and will apply to most spiking axons. We demonstrate that the essential molecular machinery can, in theory, fit into 0.06 μm diameter axons. However, a comprehensive survey of anatomical data shows a lower limit for AP-conducting axons of 0.08–0.1 μm diameter. Thus, molecular fluctuations constrain the wiring density of brains. Fluctuations have implications for epilepsy and neuropathic pain because changes in channel kinetics or axonal properties can change the rate at which channel noise generates spontaneous activity.

Results and Discussion

How Does Channel Noise Affect Signaling in Thin Axons?

The great majority of axons use action potentials (APs) to transmit information in a fast and reliable way to synapses, but, like many cell signals, the AP is generated and transmitted by a molecular mechanism that is inherently noisy. The Na and K channels open and close with probabilities that depend on membrane potential, and this stochastic behavior produces random ionic-current changes, called channel noise. Channel noise disrupts the precise timing of AP generation and could

affect systems as diverse as cortical circuits related to memory and cochlear implants [6, 7].

For propagation of the AP along an axon, Na channels act as positive feedback amplifiers, and because axonal input resistance goes as (diameter)^{-3/2} [8], the effects of single Na channels on membrane potential strongly increase as axon diameter decreases. If an axon is thin enough, a single Na channel could, in principle, generate and sustain transmission of an AP by driving the membrane to AP threshold [4, 9]. In this case, spontaneously opening Na channel will disrupt signaling by generating spontaneous action potentials (SAPs). Preliminary studies suggested a channel-noise limit to axon diameter at 0.2 and 0.3 μm [4, 5, 10]. However, many unmyelinated axons are this fine (Figure 1C), including pyramidal cell axon collaterals (average diameter 0.3 μm [1]), which form much of the local cortical circuitry, and the parallel fibers in cerebellum (average diameter 0.2 μm [11]). Yet there are no empirical data because it is difficult to record from within fine axons, and paired cell recordings cannot dissociate axonal variability from synaptic variability. We addressed this problem by developing stochastic simulations of AP propagation and supported these with analytical approximations that capture the underlying biophysics.

Stochastic Simulations

Stochastic simulations of cell signaling systems use data on the responses of individual molecules (here, the properties of ion channels) to derive the responses of systems of interacting molecules (here, the response of the axon's excitable membrane) [12] and take into account the inherent variability of molecular mechanisms. This powerful tool has proved essential for understanding and reproducing the properties of systems as diverse as vesicle exocytosis [12], cellular control of circadian rhythm [13], and cardiac activity [14]. This technique has been used to study the effects of channel noise on AP generation and neural coding (see [6] for a review), but it has usually been restricted to isopotential membrane patches [7, 15–17]. Simulating the propagation of action potentials in axons is particularly demanding because the system is highly nonlinear and spatially extensive, and just one random event, the opening of one out of many hundred thousand Na channels, can trigger a global response from the entire system. Extending a model spatially requires many compartments, and because this massively increases computational demands, there are only two published stochastic simulations of APs propagating along axons [5, 18]. We developed a fast stochastic neuron simulator, Modigliani (<http://www.modigliani.co.uk>), that incorporates special routines that increase speed and accuracy by dynamically switching stochastic integration methods to adapt to the local stochasticity of the system (see the Supplemental Data available with this article online).

As in deterministic simulators [19, 20], the axon is compartmentalized into small cylindrical segments,

*Correspondence: a.faisal@zoo.cam.ac.uk

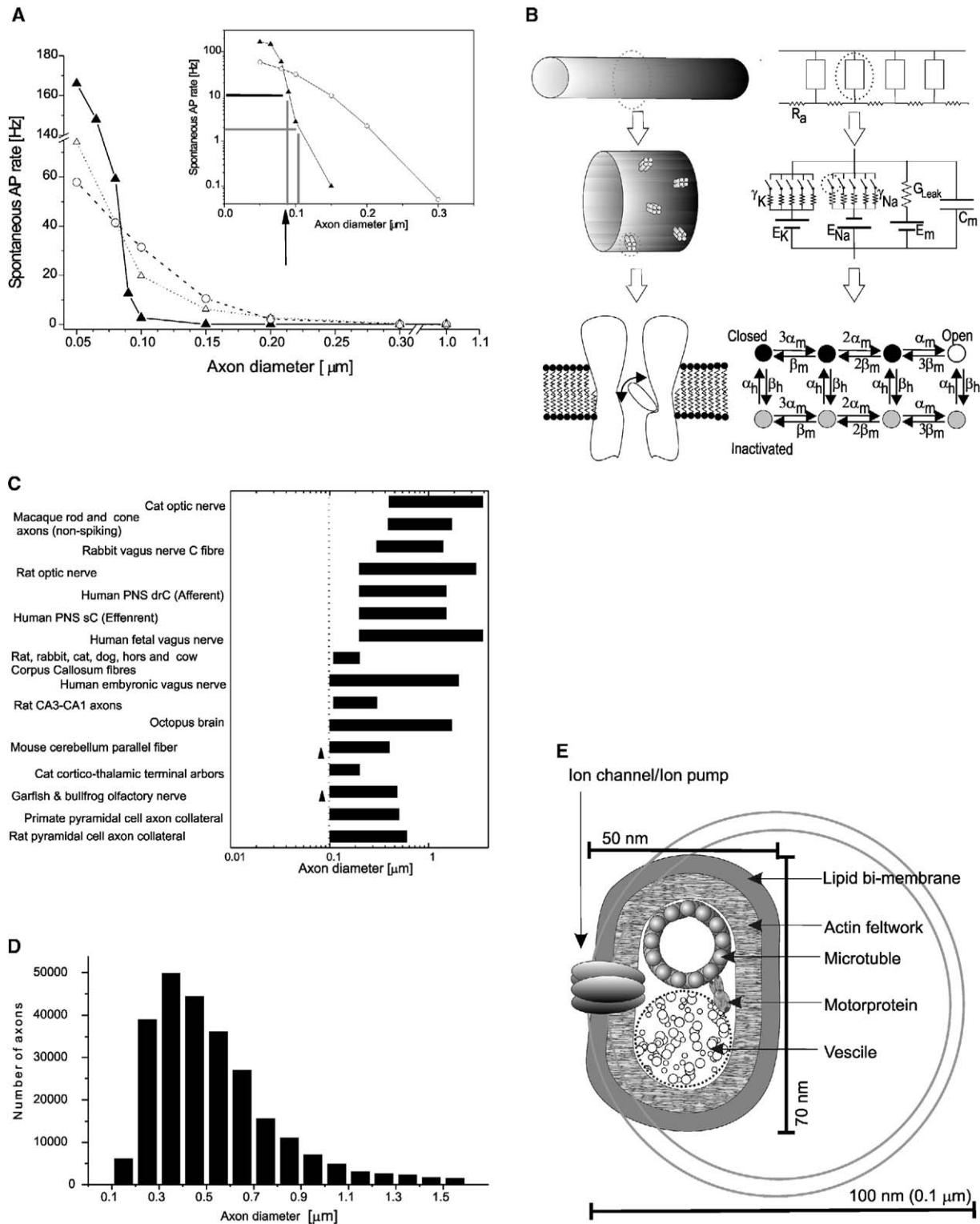


Figure 1. Molecular and Anatomical Constraints on the Diameter of Unmyelinated Axons

(A) SAP rate versus axon diameter for a pyramidal cell axon collateral (open triangles, 23°C; closed triangles, 37°C) and a squid axon (circle) of 1 mm length. Spontaneous AP rate increases sharply below a critical diameter of 0.15–0.2 μm . (Inset) Semilogarithmic plot of the data shows the exponential character of the dependence of spontaneous AP rate on diameter below the critical diameter. The arrow highlights how little changing the signal AP rate from 4 to 20 Hz affects the limiting diameter (the diameter at which SAP rate equals half the signal AP rate). (B) The stochastic axon simulator (see [Supplemental Data](#) for details). (Top) The axon is a sequence of cylindrical segments. (Middle) Each segment of axon membrane contains two populations of ion channels. (Bottom) An ion channel is modeled with a finite-state Markov random

modeled as a series of transmembrane electrical circuits coupled intracellularly by axoplasmic resistance (R_a) and extracellularly by a negligible resistance (Figure 1B). The membrane of each axon segment contains two populations of identified ion channels, voltage-sensitive sodium channels (Na), and delayed-rectifier potassium channels (K) and is modeled as an equivalent electrical circuit with a membrane capacitance (C_m) and a leak conductance ($g_{Leak} = 1/R_{Leak}$). Each ion channel corresponds to a switch in series with the single-channel conductance (γ_i) and a battery representing the equilibrium potential (E_i) of the channel's ionic species. The opening and closing of every ion channel is modeled with Markov random process, reflecting discrete states of the channel protein [21]. State-transition probabilities are given by kinetic-rate functions $\alpha(V)$, $\beta(V)$, which depend instantaneously on the axon segment's membrane potential V (Tables S1 and S2) [21]. In the limit of large numbers of ion channels per unit length of axon—that is, axons of diameter above 1 μm —the stochastic model converges to a deterministic Hodgkin-Huxley-type model.

We ignored the membrane's Johnson and shot noise (three orders of magnitude weaker than channel noise [22]).

Spontaneous Activity and Diameter in Cortical and Squid Axons

To establish quantitative relationships between diameter and SAP rate, we examined two very different axons. Firstly, the rodent cortical pyramidal cell axon collateral was modeled at 23°C and 37°C with putative kinetic models for the $\text{Na}_v1.2$ and $\text{K}_v1.1/2$ ion channels. With a total length of about 4 cm per pyramidal cell, this axon forms the great majority of the connections in local cortical networks [1]. Secondly, squid axon was simulated at 6.3°C with putative kinetic models for the GFLN1 and SqKv1A ion channels because squid axon is arguably the best-studied neuronal signaling system. In squid, we also used alternative, more complex kinetic models of the same ion channel, but we found no significant differences in the results. Both axon models are defined by their characteristic sets of biophysical parameters and ion-channel kinetics (see Tables S1 and S2). We varied these parameter sets and the ion-channel kinetics in both models to test parameter sensitivity and thereby implicitly covered a wide range of axons. Because no external current, such as synaptic input, was applied to the model axons, all resulting APs are spontaneous events triggered by channel noise.

Our simulations show that in both types of axon, significant numbers of SAPs start to appear (>0.02 SAP/s) at a critical diameter of 0.15–0.3 μm (Figure 1A). These

values are considerably lower than previous theoretical estimates because we used newer data on single-channel properties [4] and more accurate models of channel kinetics [5], which accounts for the different closed states of ion channels in our simulations. Below the critical diameter, SAP rate increases exponentially (Figure 1A, inset), to the point where the axon's refractory period limits SAP rate and it levels off. Above the critical diameter, SAPs become increasingly unlikely (in our simulations, <0.2 SAP/s) because the number n of open channels required to trigger an AP increases as $d^{3/2}$, and the probability of n close-by channels being open decreases in proportion to the n -th power of the probability that a single channel is open.

Underlying Biophysics of Spontaneous APs

The exponential dependence of spontaneous rate on axon diameter follows from basic biophysics. Spontaneously open Na channels generate a depolarizing current (Figure 2B) that charges the membrane (Figure 2A) in proportion to the current's size and duration and in proportion to the membrane's input resistance. Because input resistance increases with decreasing diameter, the number of nearby simultaneously open channels required to charge the membrane to AP threshold falls. At the critical diameter, a single open Na channel can trigger a SAP (Figure 2A, black arrowhead) if it stays open long enough. Below the critical diameter, the SAP rate increases steeply because channel open times are exponentially distributed. Consequently, the probability that a Na channel remains open long enough to trigger an AP also increases exponentially as diameter decreases (see Figure 1A).

To validate the simulations and to understand the dependence of channel-noise effects on biophysical parameters, we derive two approximate formulas that bracket the exact solution by under- and overestimating the true value (for details, see Supplemental Data; an exact analytical expression is mathematically intractable because the effects of small numbers of channels in a highly nonlinear system are considered).

First, in the limit of large numbers of channels, stochastic transmembrane current can be described by continuous Gaussian processes that are defined by channel kinetics near the resting potential (i.e., we assume there is no cooperativity between channels). Applying this noise current to the cable model of a resting axon, we calculate the membrane potential noise and estimate how often it crosses AP threshold. This approximation shows that SAP rate increases exponentially with decreasing diameter and places the critical diameter at 0.06–0.08 μm . This Gaussian approximation underestimates the SAP rate and critical diameter

process, reflecting discrete states of the channel protein. We depict here the Na channel model, which has a single open state, three closed, and four inactivated states [21]. Similarly, the K channel Markov model (not shown) has a single open state and four closed states [21].

(C) Diameters of fine AP-conducting axons in a wide range of species and tissues [1–3, 26, 36, 43–51]. The finest AP-conducting axons reach the limiting diameter of 0.1 μm (dotted line); the few exceptions are developing fibers of 0.08 μm diameter (arrowhead).

(D) Diameter distribution of over 250,000 axons in octopus brain. Data extracted from [26].

(E) Scale drawing illustrating how essential components can be packed into the cross-section of an axon of 50 nm diameter (see text for details). The unfilled circle illustrates the finest known AP-conducting axons, whose diameter, 100 nm, corresponds to the channel-noise limit derived in this study.

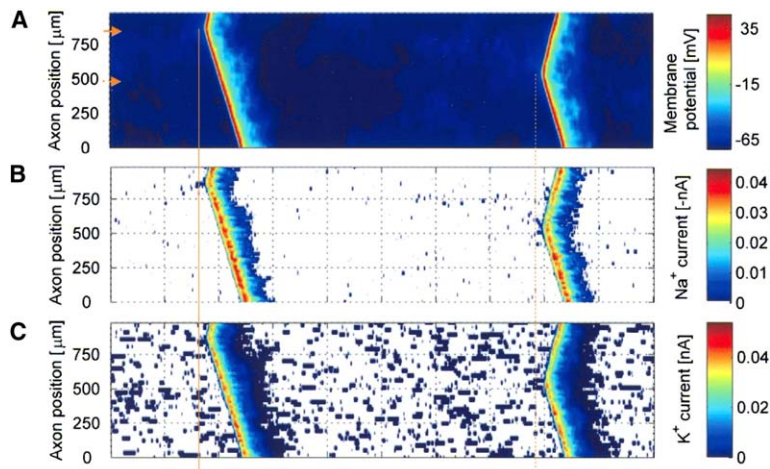


Figure 2. The Generation and Propagation of SAPs

(A–C) Space-time plots of membrane potential (A) and transmembrane Na⁺ and K⁺ currents (B and C) in a simulation of a 1-mm-long pyramidal cell axon collateral ($d = 0.1 \mu\text{m}$) at 23°C. In (B) and (C), the regions where no transmembrane current was flowing were not color coded, making ionic currents from spontaneously open channels clearly visible. The prolonged open time of single Na channels at $t = 15 \text{ ms}$ and $t = 77 \text{ ms}$ depolarizes the membrane to AP threshold, recruiting several nearby channels and resulting in spontaneous APs, at $t = 17 \text{ ms}$ and $t = 79 \text{ ms}$, that subsequently propagate along the axon. The AP waveform (see also Figure S3B) and the corresponding ionic current traces match empirical data and deterministic simulations (data not shown). Horizontal (time) axis divisions are 10 ms.

because channel numbers are very small, and the depolarizing current steps produced by individual ion channels are large in comparison to the smooth Gaussian process.

The second approximation assumes that small numbers of ion channels produce discrete changes in current, but it ignores their stochastic behavior, and one determines how many channels have to simultaneously open (and stay open long enough) to trigger an AP for a given set of axon properties and diameter. This suggests that a single Na channel can trigger SAPs in axons below 0.15–0.3 μm diameter, but because channel open times are random, this approximation yields an upper limit to SAP rates.

Our two analytical approximations place the critical axon diameter between 0.06 and 0.3 μm . As expected from the observation that one approximation underestimates, the other overestimates, and the simulations yield an exact numerical solution, the critical diameters determined by our stochastic simulation lie inside this range.

In conclusion, basic biophysical theory shows that the increase in SAP rate below the critical diameter is an inevitable consequence of the design of the AP signaling mechanism and explains how the critical diameter at which SAPs start to appear is set by the biophysical parameters of the axon. Our stochastic stimulations establish that the mammalian pyramidal cell axon and the squid axon have critical diameters of 0.15 μm and 0.2 μm (Figure 1A, vertical gray lines), and this similarity suggests that an axon’s critical diameter is relatively insensitive to changes in its biophysical parameters.

Sensitivity to Biophysical Parameters

Both mammalian pyramidal cells and squid axons yield similar results (Figure 1A), and this suggests that the critical diameter is relatively insensitive to biophysical parameters. Our formulas show that the critical diameter depends on the cubed root of the specific membrane resistance and axoplasmic resistance ($d_{crit} \sim R_m$, $d_{crit} \sim R_a$) and as the two third power of both the number of simultaneously open Na⁺ channels per electrotonic unit of axon (this number covaries with

channel density) and the single-channel conductance ($d_{crit} \sim n_0^{2/3}$, $d_{crit} \sim \gamma_{Na}^{2/3}$). These are weak (i.e., strongly sublinear) dependencies. The orders of magnitude of these key parameters are constrained by the properties of the basic nerve-cell constituents, such as the membrane bilayer and the resistance of the cytoplasm used as the conducting core. These parameters have more effect on the critical diameter than factors such as the detailed kinetic scheme of channels; consequently, the majority of axons will have critical diameters on the order of 0.1 μm .

Stochastic simulations confirm that the critical diameter is relatively insensitive to varying biophysical parameters over a biologically plausible range (for detailed discussion and data, see Supplemental Data). We focused on changes that can decrease SAP rate because the nervous system might exploit these to construct finer-diameter axons with lower SAP rates. Varying Na channel conductance (four orders of magnitude; Figure S1), membrane resistance ($\pm 75\%$; Figure S2A), the axoplasmic resistance ($\pm 75\%$; Figure S2B), and the Na channel and K channel densities (both $\pm 75\%$; Figures S2C and S2D) and membrane capacitance ($\pm 50\%$; Figure S4) does not substantially reduce the SAP rate without either significantly exceeding the known biological range of parameters or degrading the reliability of AP transmission by reducing membrane excitability. We also compared the behavior of axons with stochastic Na channels and deterministic K channels and vice versa to establish that the major cause of SAPs is Na channel noise (see Figure S5). Finally, we established that the gating current, caused by the movement of polarized domains in the channel protein, has only a small effect on SAP rate ($< 14\%$; see Supplemental Data).

All our parameter variations, including temperature (below), change the SAP rate at a given diameter by shifting the exponential curve of SAP rate against diameter or altering its exponent slightly. However, the exponential nature of this relationship is unaffected because it results from three basic biophysical properties of AP signaling: the exponential distribution of channel open times, the increase in input resistance with decreasing axon diameter, and a voltage threshold. We conclude

that the relationship between channel noise and critical diameter is robust, and most types of unmyelinated axons will have similar critical diameters.

Increasing Temperature Decreases Noise from Spontaneous Activity

We find that temperature has a counterintuitive effect on spontaneous activity. The SAP rate is inversely temperature dependent in the cortical pyramidal cell and the squid axon, which operate at very different temperatures (Figure 1A; Figure S3). In our pyramidal axon model, the critical diameter fell from 0.2 to 0.15 μm when temperature was increased from 23°C to 37°C (Figure S3A). Spontaneous activity falls with increasing temperature because when ion-channel kinetics speed up, the duration of spontaneous depolarizing currents decreases, and the membrane is, therefore, less likely to reach AP threshold. In other words, increasing temperature shifts channel noise to higher frequencies, at which it is attenuated by the low pass characteristics of the axon [23]. This effect of shorter channel open times prevails over the increased rate of spontaneous channel openings.

Neuroanatomy and the Limits to Axon Diameter

The exponential increase of SAP rate below the critical diameter of 0.15–0.2 μm limits the ability of thinner axons to transmit information. Signal APs generated by synaptic inputs at the proximal end of the axon will mix and interact with SAPs on their way to the output synapses. The limiting diameter below which the SAP rate becomes intolerable for communication depends only weakly on the AP rate used for communication because SAP rate increases very steeply below the critical diameter. Varying the signaling rate in a pyramidal cell from 4 to 20 Hz only shifts the limiting diameter (here, the diameter at which SAP rate is half the signal AP rate) from 0.1 to 0.09 μm (see Figure 1A, arrow). Mean signal AP rates of 1–10 Hz in cortical neurons [8, 24, 25] suggest a limiting diameter of $\sim 0.1 \mu\text{m}$.

Reviewing high-resolution electron-micrograph studies covering several taxa and including a comprehensive survey of over 250,000 axons in octopus [26], we consistently found a minimum axon diameter of 0.1 μm , with rare exceptions down to 0.08 μm in possibly developing, electrically passive axons (Figure 1C). The axon-diameter distributions that reach 0.1 μm are skewed, typically peak at 0.3–0.5 μm , and fall off sharply to zero at or just below 0.1 μm (Figure 1D and data in references of Figure 1C). This suggests that axon diameters are pushed toward the channel-noise limit of 0.1 μm .

Steric Limits to Axon Miniaturization

We use a volume exclusion argument to show that it is possible to construct axons much finer than 0.1 μm (Figure 1E). Neural membrane (5 nm thickness) can be bent to form axons of 30 nm diameter because it also forms spherical synaptic vesicles of that diameter. A few essential molecular components are required to fit inside the axon; this includes an actin filament (7 nm thick) to support membrane shape, the supporting cytoskeleton (a microtubule of 23 nm diameter), the intra-

cellular domains of ion channels and pumps (intruding 5–7 nm), and kinesin motor proteins (10 nm length) that transport vesicles (30 nm diameter) and essential materials (<30 nm diameter) [27]. Adding up the cross-sectional areas shows that it is possible to pack these components into axons as fine as 0.06 μm (=60 nm). Indeed, the finest known neurites, those of amacrine cells in *Drosophila* lamina, are about 0.05 μm in diameter, contain microtubules, and connect to extensive dendritic arbors but do not transmit APs [28, 29]. The fact that the smallest known AP-conducting axons are about twice as large as the steric limit to axon diameter (0.1 μm cf. 0.06 μm) (Figure 1E), whereas electrically passive axons reach the physical limit, supports our argument that channel noise limits the diameter of AP-conducting axons to about 0.1 μm .

Limits to Miniaturization of the Brain's Wiring

The small diameter and high density of neurons in brains suggest that miniaturization improves efficiency. Engineers miniaturize computer chips to reduce energy consumption, transmission times, weight, and size, and similar considerations apply to nervous systems. There are definite indications that nervous systems have evolved to minimize wiring costs [30–33], and miniaturization can reduce size, transmission times [32], and the substantial quantity of energy used to transmit electrical signals [24] by reducing axon diameter, length, and, hence, membrane surface area. We estimated that nervous systems can achieve component and cabling densities over three orders higher than circuits in computer chips (see Supplemental Data), and many populations of axons have diameter distributions that are skewed toward and touch the channel-noise limit (Figure 1D and data in references of Figure 1C). These observations suggest that an evolutionary drive toward miniaturization is limited by channel-noise effects. Apparently, the brain cannot shrink its wiring much below 0.1 μm because it uses a self-regenerating electrical signal, amplified by voltage-sensitive protein switches prone to thermodynamic fluctuations, and these proteins are placed in a lipid-insulated cable with an aqueous conducting core. Thus, the high electrical resistance of cytoplasm not only necessitates the use of APs [34] but also limits axon diameter. We note that when we apply the same biophysical considerations to spherical neurons with axon-like excitable membrane, this suggests a lower limit to soma diameter of about 4 μm , which is approached by the somata of cerebellar granule cells.

Channel noise is not the only constraint to axon diameter. Many unmyelinated axons, especially in sensory and motor systems, have diameters above the channel-noise limit (Figure 1C). Besides increased AP conduction velocity, thicker axons can support higher AP rates. This is because with a lower surface-area-to-volume ratio, they provide better buffering against the ion-concentration changes produced by APs [35] and can accommodate more sources and buffering of energy for ion pumping. Axon diameter also increases with the number and activity of output synapses, possibly to support higher rates of axoplasmic transport [36].

Ion-Channel Diversity and the Channel-Noise Limit

Axon diameter is constrained to about 0.1 μm , within the known set of ion-channel conductances and open times. This raises the question, Why are these channel properties as they are? A key property is the voltage-gated channel conductance, which is typically in the range of 5–50 pS (based on unitary channel measurements), well below the theoretical upper limit of 300 pS [21]. Na channel conductances show an even smaller range of 15–25 pS [21]. Perhaps unidentified requirements set the minimum diameter of axons to 0.1 μm , and ion channels evolved to work within this limit? Given that the same ion channels are used in both large- and small-diameter axons, this seems unlikely, but at the moment we cannot decide.

Nonetheless, our findings raise the possibility that voltage-sensitive channels have diversified to improve the reliability and efficiency of fine axons. Although the SAP rate is relatively insensitive to channel properties' parameters, it does change (see parameter variations in the [Supplemental Data](#)), and this suggests that variations in the channel mix in fine axons could improve, or in pathological cases decrease, overall reliability. The changes in reliability we observed are small (two types of Na channels, the cortical Nav1.2 and the squid GFLN, produce similar noise effects), but could more reliable ion channels with drastically different properties lower the limit to axon diameter? In principle, increasing the amount of energy required to open a channel by increasing its gating charge would lower the probability that it opens spontaneously. However, reliability comes at a price. Increasing the switching threshold reduces the safety factor for conduction and the AP propagation speed and increases the cost of generating an action potential with synaptic input. Similarly, an increased inactivation speed, such as in the sodium channel Nav1.6, predominantly found in Nodes of Ranvier [37], would require higher channel densities to maintain the safety factor for conduction.

Conclusions

Stochastic simulations, supported by simple biophysical theory and parameter variations, show how noise generated by ion channels produces spontaneous APs in fine axons. This molecular noise places a lower limit to axon diameter, 0.1 μm , which is close to that observed anatomically. From a biomedical perspective, these biophysically realistic stochastic simulations provide a promising way to study the functional significance of mixing different ion channels in fine nociceptive fibers [38] and of investigating the effects of ion-channel mutations associated with epilepsy [39, 40] on spontaneous activity [41]. From an evolutionary perspective, being warm-blooded not only increases the speed of neural processing, but it also improves reliability and allows the use of smaller structures. However, the extent of this advantage remains unclear because ion-channel kinetics can be adapted to body temperature [42]. From a systems perspective, our study shows how the noisiness of the protein switches used for amplification imposes a lower limit to the miniaturization of a cell signaling system. This molecular noise makes electrical signaling unfeasible at the

nanometer scale both for cells and for nanotechnology based on such biomolecular components. We pose the question of which kind of signaling mechanisms are most appropriate for fast and reliable signaling on a given length scale, and we note that on the submicron scale, cells prefer chemical and mechanical signaling mechanisms over electrical ones.

Supplemental Data

Supplemental Results and Discussion, as well as several supplemental figures and tables, are available at <http://www.current-biology.com/cgi/content/full/15/12/1143/DC1/>.

Acknowledgments

We thank William Bialek, Graeme Mitchison, and Gordon Shepherd for stimulating discussions, John Messenger for providing the octopus data set collected by J.-P. Camm, and Dennis Bray, Malcolm Burrows, and an anonymous referee for comments on the manuscript. A.A.F. is a Boehringer-Ingelheim Fonds PhD scholar, a Biotechnology and Biological Sciences Research Council (BBSRC)-supported research student, and a nonstipendiary scholar of the Studienstiftung des deutschen Volkes. J.A.W. was supported by a Research Travel Grant from the Burroughs-Wellcome Foundation, by a by-Fellowship from Churchill College, Cambridge, and by grants from the National Institutes of Health and National Science Foundation. S.B.L. is supported by the Rank Prize Fund and the BBSRC.

Received: January 10, 2005

Revised: May 9, 2005

Accepted: May 10, 2005

Published: June 21, 2005

References

1. Braitenberg, V., and Schüz, A. (1998). *Statistics and Geometry of Neuronal Connectivity*, Second Edition (Berlin: Springer).
2. Heck, D., and Sultan, F. (2002). Cerebellar structure and function: Making sense of parallel fibers. *Hum. Mov. Sci.* 27, 411–421.
3. Berthold, C.-H. (1978). Morphology of normal peripheral axons. In *Physiology and Pathobiology of Axons*, S.G. Waxman, ed. (New York: Raven Press), pp. 3–63.
4. Hille, B. (1970). Ionic channels in nerve membranes. *Prog. Biophys. Mol. Biol.* 21, 3–28.
5. Horikawa, Y. (1991). Noise effects on spike propagation in the stochastic Hodgkin-Huxley models. *Biol. Cybern.* 66, 19–25.
6. White, J.A., Rubinstein, J.T., and Kay, A.R. (2000). Channel noise in neurons. *Trends Neurosci.* 23, 131–137.
7. Schneidman, E., Freedman, B., and Segev, I. (1998). Ion channel stochasticity may be critical in determining the reliability and precision of spike timing. *Neural Comput.* 10, 1679–1703.
8. Koch, C. (1999). *Biophysics of Computation* (Oxford: Oxford University Press).
9. Waxman, S.G., Black, J.A., Kocsis, J.D., and Ritchie, J.M. (1989). Low density of sodium channels supports action potential conduction in axons of neonatal rat optic nerve. *Proc. Natl. Acad. Sci. USA* 86, 1406–1410.
10. Franciolini, F. (1987). Spontaneous firing and myelination of very small axons. *J. Theor. Biol.* 128, 127–134.
11. Sultan, F. (2000). Exploring a critical parameter of timing in the mouse cerebellar microcircuitry: The parallel fiber diameter. *Neurosci. Lett.* 280, 41–44.
12. Franks, K.M., Stevens, C.F., and Sejnowski, T.J. (2003). Independent sources of quantal variability at single glutamatergic synapses. *J. Neurosci.* 23, 3186–3195.
13. Barkai, N., and Leibler, S. (2000). Circadian clocks limited by noise. *Nature* 403, 267–268.
14. Tan, H.L., Bink-Boelkens, M.T.E., Bezzina, C.R., Viswanathan, P.C., Beaufort-Krol, G.C.M., van Tintelen, P.J., van den Berg,

- M.P., Wilde, A.A.M., and Balsler, J.R. (2001). A sodium-channel mutation causes isolated cardiac conduction disease. *Nature* 409, 1043–1047.
15. Skaugen, E., and Walløe, L. (1979). Firing behaviour in a stochastic nerve membrane model based upon the Hodgkin-Huxley equations. *Acta Physiol. Scand.* 107, 343–363.
 16. Lecar, H., and Nossal, R. (1971). Theory of threshold fluctuations in nerves: 1. Relationships between electrical noise and fluctuations in axon firing. *Biophys. J.* 11, 1049–1067.
 17. Strassberg, A.F., and DeFelice, L.J. (1993). Limitations of the Hodgkin-Huxley formalism: Effects of single channel kinetics upon transmembrane voltage dynamics. *Neural Comput.* 5, 843–855.
 18. Adair, R.K. (2003). Noise and stochastic resonance in voltage-gated ion channels. *Proc. Natl. Acad. Sci. USA* 100, 12099–12104.
 19. Hines, M.L., and Carnevale, N.T. (1997). The NEURON simulation environment. *Neural Comput.* 9, 1179–1209.
 20. Bower, J.M., and Beeman, D. (1998). *The Book of GENESIS: Exploring Realistic Neural Models with the GENeral NEural Simulation System*, Second Edition (New York: TELOS/Springer-Verlag).
 21. Hille, B. (2001). *Ion Channels of Excitable Membranes* (Sunderland, MA: Sinauer Associates).
 22. Manwani, A., and Koch, C. (1999). Detecting and estimating signals in noisy cable structures. I. Neuronal noise sources. *Neural Comput.* 11, 1797–1829.
 23. Steinmetz, P.N., Manwani, A., Koch, C., London, M., and Segev, I. (2000). Subthreshold voltage noise due to channel fluctuations in active neuronal membranes. *J. Comput. Neurosci.* 9, 133–148.
 24. Attwell, D., and Laughlin, S.B. (2001). An energy budget for signalling in the grey matter of the brain. *J. Cereb. Blood Flow Metab.* 21, 1133–1145.
 25. Baddeley, R., Abbott, L.F., Booth, M.C., Sengpiel, F., Freeman, T., Wakeman, E.A., and Rolls, E.T. (1997). Responses of neurons in primary and inferior temporal visual cortices to natural scenes. *Proc. R. Soc. Lond. B. Biol. Sci.* 264, 1775–1783.
 26. Camm, J.-P. (1986). *The chromatophore lobes and their connections in octopus*. PhD thesis, University of Sheffield, Sheffield, UK.
 27. Alberts, B., Johnson, A., Lewis, J., Raff, M., Roberts, K., and Walter, P. (2002). *Molecular Biology of the Cell* (New York: Garland).
 28. Shaw, S.R. (1981). Anatomy and physiology of identified non-spiking cells in the photoreceptor-lamina complex of the compound eye of insects, especially Diptera. In *Neurons without Impulses*, A. Roberts and B.M.H. Bush, eds. (Cambridge: Cambridge University Press), pp. 61–66.
 29. Meinertzhagen, I.A., and O’Neil, S.D. (1991). Synaptic organization of columnar elements in the lamina of the wild-type in *Drosophila melanogaster*. *J. Comp. Neurol.* 305, 232–263.
 30. Ramon y Cajal, S. (1995). *Histology of the Nervous System of Man and Vertebrates*, Volume 1 (New York: Oxford University Press).
 31. Cherniak, C. (1994). Component placement optimization in the brain. *J. Neurosci.* 14, 2418–2427.
 32. Chklovskii, D.B., Schikorski, T., and Stevens, C.F. (2002). Wiring optimization in cortical circuits. *Neuron* 34, 341–347.
 33. Chklovskii, D.B., and Koulakov, A.A. (2004). Maps in the brain: What can we learn from them? *Annu. Rev. Neurosci.* 27, 369–392.
 34. Hodgkin, A.L. (1964). *The Conduction of the Nervous Impulse* (Liverpool, UK: Liverpool University Press).
 35. Qian, N., and Sejnowski, T.J. (1989). An electro-diffusion model for computing membrane potentials and ionic concentrations in branching dendrites, spines and axons. *Biol. Cybern.* 62, 1–15.
 36. Hsu, A., Tsukamoto, Y., Smith, R.G., and Sterling, P. (1998). Functional architecture of primate cone and rod axons. *Vision Res.* 38, 2539–2549.
 37. Caldwell, J.H., Schaller, K.L., Lasher, R.S., Peles, E., and Levinson, S.R. (2000). Sodium channel Na(v)1.6 is localized at nodes of ranvier, dendrites, and synapses. *Proc. Natl. Acad. Sci. USA* 97, 5616–5620.
 38. Fang, X., Djouhri, L., Black, J.A., Dub-Hajj, S.D., Waxman, S.G., and Lawson, S.N. (2002). The presence and role of the tetrodotoxin-resistant sodium channel Na_v1.9 (NaN) in nociceptive primary afferent neurons. *J. Neurosci.* 22, 7425–7433.
 39. Hirose, S., Okada, M., Yamakawa, K., Sugawara, T., Fukuma, G., Ito, M., Kaneko, S., and Mitsudome, A. (2002). Genetic abnormalities underlying familial epilepsy syndromes. *Brain Dev.* 24, 211–222.
 40. Kohling, R. (2002). Voltage-gated sodium channels in epilepsy. *Epilepsia* 43, 1278–1295.
 41. Lossin, C., Wang, D.W., Rhodes, T.H., Vanoye, C.G., and George, A.L., Jr. (2002). Molecular basis of an inherited epilepsy. *Neuron* 34, 877–884.
 42. Rosenthal, J.J., and Bezanilla, F. (2000). Seasonal variation in conduction velocity of action potentials in squid giant axons. *Biol. Bull.* 199, 135–143.
 43. Williams, R.W., and Chalupa, L.M. (1983). An analysis of axon caliber within the optic nerve of the cat: Evidence of size groupings and regional organization. *J. Neurosci.* 3, 1554–1564.
 44. Keynes, R.D., and Ritchie, J.M. (1965). The movements of labelled ions in mammalian non-myelinated nerve fibres. *J. Physiol.* 179, 333–367.
 45. Sugimoto, T., Fukuda, Y., and Wakakuwa, K. (1984). Quantitative analysis of a cross-sectional area of the optic nerve: A comparison between albino and pigmented rats. *Exp. Brain Res.* 54, 266–274.
 46. Wozniak, W., and O’Rahilly, R. (1981). Fine structure and myelination of the developing human vagus nerve. *Acta Anat. (Basel)* 109, 218–230.
 47. Olivares, R., Montiel, J., and Aboitiz, F. (2001). Species differences and similarities in the fine structure of the mammalian corpus callosum. *Brain Behav. Evol.* 57, 98–105.
 48. Shepherd, G.M., and Harris, K.M. (1998). Three-dimensional structure and composition of CA3-CA1 axons in rat hippocampal slices: Implications for presynaptic connectivity and compartmentalization. *J. Neurosci.* 18, 8300–8310.
 49. Guillery, R.W., Feig, S.L., and van Lieshout, D.P. (2001). Connections of higher order visual relays in the thalamus: A study of corticothalamic pathways in cats. *J. Comp. Neurol.* 438, 66–85.
 50. Easton, D.M. (1971). Garfish olfactory nerve: Easily accessible source of numerous long, homogeneous nonmyelinated axons. *Science* 172, 952–955.
 51. Small, R.K., and Pfenninger, K.H. (1984). Components of the plasma membrane of growing axons. 1. Size and distribution of intramembrane particles. *J. Cell Biol.* 98, 1422–1433.